

ARMY RESEARCH LABORATORY



A Novel Thermal Management Approach for Radial Foil Air Bearings

by Kevin Radil and CDT Zach Batcho

ARL-MR-0749

July 2010

NOTICES

Disclaimers

The findings in this report are not to be construed as an official Department of the Army position unless so designated by other authorized documents.

Citation of manufacturer's or trade names does not constitute an official endorsement or approval of the use thereof.

Destroy this report when it is no longer needed. Do not return it to the originator.

Army Research Laboratory

NASA Glenn, Cleveland, OH 44135-3191

ARL-MR-0749

July 2010

A Novel Thermal Management Approach for Radial Foil Air Bearings

Kevin Radil
NASA Glenn Research Center
Cleveland, OH

and

CDT Zach Batcho
U.S. Military Academy
West Point, NY

REPORT DOCUMENTATION PAGE

Form Approved
OMB No. 0704-0188

Public reporting burden for this collection of information is estimated to average 1 hour per response, including the time for reviewing instructions, searching existing data sources, gathering and maintaining the data needed, and completing and reviewing the collection information. Send comments regarding this burden estimate or any other aspect of this collection of information, including suggestions for reducing the burden, to Department of Defense, Washington Headquarters Services, Directorate for Information Operations and Reports (0704-0188), 1215 Jefferson Davis Highway, Suite 1204, Arlington, VA 22202-4302. Respondents should be aware that notwithstanding any other provision of law, no person shall be subject to any penalty for failing to comply with a collection of information if it does not display a currently valid OMB control number.

PLEASE DO NOT RETURN YOUR FORM TO THE ABOVE ADDRESS.

1. REPORT DATE (DD-MM-YYYY) July 2010		2. REPORT TYPE Final		3. DATES COVERED (From - To) June 2009 to August 2009	
4. TITLE AND SUBTITLE A Novel Thermal Management Approach for Radial Foil Air Bearings				5a. CONTRACT NUMBER	
				5b. GRANT NUMBER	
				5c. PROGRAM ELEMENT NUMBER	
6. AUTHOR(S) Kevin Radil and CDT Zach Batcho				5d. PROJECT NUMBER	
				5e. TASK NUMBER	
				5f. WORK UNIT NUMBER	
7. PERFORMING ORGANIZATION NAME(S) AND ADDRESS(ES) U.S. Army Research Laboratory NASA Glenn ATTN: RDRL-VTP Cleveland, OH 44135-3191				8. PERFORMING ORGANIZATION REPORT NUMBER ARL-MR-0749	
9. SPONSORING/MONITORING AGENCY NAME(S) AND ADDRESS(ES)				10. SPONSOR/MONITOR'S ACRONYM(S)	
				11. SPONSOR/MONITOR'S REPORT NUMBER(S)	
12. DISTRIBUTION/AVAILABILITY STATEMENT Approved for public release; distribution unlimited.					
13. SUPPLEMENTARY NOTES					
14. ABSTRACT We experimentally evaluated a novel thermal management technique for radial foil air bearings. The technique is based on injecting air directly into the internal circulating fluid-film to reduce bulk temperatures and axial thermal gradients. The tests were performed on a single top foil, Generation III, radial foil bearing instrumented with three thermocouples to monitor internal temperatures. A thru hole in the bearing shell coincident with the gap between the top foil's fixed and free ends provided entry for the injection air. The tests were conducted at room temperature with the bearing operating at speeds from 20 to 50 krpm while supporting 222N. Two different mass flow rates of injection air were evaluated for this method, 0.017 and 0.051 kg/min. Test results suggest that the air injection approach is a viable thermal management technique capable of controlling bulk temperatures and axial thermal gradients in radial foil air bearings.					
15. SUBJECT TERMS Foil air bearing, gas bearing, turbomachinery					
16. SECURITY CLASSIFICATION OF:			17. LIMITATION OF ABSTRACT UU	18. NUMBER OF PAGES 22	19a. NAME OF RESPONSIBLE PERSON Kevin Radil
a. REPORT Unclassified	b. ABSTRACT Unclassified	c. THIS PAGE Unclassified			19b. TELEPHONE NUMBER (Include area code) (216) 433-5047

Contents

List of Figures	4
List of Tables	4
1. Introduction	5
2. Test Apparatus	9
3. Procedure	11
4. Test Results and Discussion	11
5. Conclusion	16
6. References	17
Distribution List	19

List of Figures

Figure 1. Schematic of the test bearing showing locations of thermocouples and inlet hole for air injection.....	9
Figure 2. Hardware layout for injecting air into the bearing.	10
Figure 3. High-speed, high-temperature, journal foil air bearing test rig.....	11
Figure 4. Time history plot of bearing temperatures and maximum axial thermal gradient showing the effects of applying air injection flows of 0.017 and 0.051 kg/min. Speed = 30 krpm, load = 222N.	13
Figure 5. Bearing temperatures demonstrating an excessive thermal gradient situation. Injection air at 0.051 kg/min was delivered at the 3.5 min mark followed by 0.068 kg/min at the 4.5 min mark. Test was discontinued once the thermal gradient surpassed 25 °C/cm. Speed = 50 krpm. Load = 89N.	14
Figure 6. Repeat of operating conditions that led to failure (figure 5) except a constant air injection of 0.068 kg/min was applied at the beginning of the test. Speed = 50 krpm. Load = 89N.	14

List of Tables

Table 1. Bearing temperature results for the two injection air flows at three different operating speeds while supporting 222N. Injection air temperature = 23 °C.....	12
Table 2. Effect of air injection location with respect to the load support region on bearing temperatures and thermal gradient. Speed = 20 krpm. Load = 89N. Injection air temperature = 22 °C.....	15

1. Introduction

Foil bearings are hydrodynamic bearings that generate a thin gas film ($\sim 10^{-5}$ m) from the natural pumping action of a rotating shaft that drags air into a convergent wedge-shaped gap to produce pressure. The basic elements of a foil air bearing are the shell, top foil, and bump foils. The top foil is a thin flexible membrane that retains the generated fluid pressure and is supported by elastic support structures called bump foils. Bump foils are shaped similar to the corrugations in a cardboard box with each bump acting as a structural spring that allows the top foil to move in response to hydrodynamic pressure changes due to static and dynamic loads, shaft centrifugal and thermal growth, and misalignment. Bump foils are also responsible for the bearing's stiffness and damping properties and can be adjusted for specific applications through their judicious design. The material of choice for foil bearings is typically a nickel based superalloy because of its high temperature stiffness properties but other materials, chosen with respect to operating requirements and conditions, may also be used.

The concept of a foil bearing was first described in a report over 50 years ago by Blok and Van Rossum (1). Since their discovery, foil bearings have been commonly used as rotor supports in air cycle machines (ACM's) that are part of an aircraft's cabin environmental system (2). This application is relatively benign and requires only simple bump foil designs because speeds are high and temperatures and loads are low. Transitioning these simple designed foil bearings into more complex systems was subsequently attempted but progressed no further than the research stage (3, 4). However, during the last 15 years, more advanced, higher load capacity bearings and high temperature coatings for wear protection have been developed, driving the technology into larger, more demanding systems. Current Oil-Free commercial products using advanced bearings include 60 and 200 kW microturbines for power generation and air compressors (5). Recent industrial research activities are suggesting that future Oil-Free turbomachinery will also include turbochargers, larger microturbines, auxiliary power units (APU's) and gas turbine engines (6, 7).

With air as the lubricant, foil bearings can successfully support high speed rotors in extreme temperature environments without the threat of fluid degradation. The ability to operate at high temperature, however, does not preclude them from having their own unique thermal management issues that require attention during the design of an Oil-Free system. The thermal profile in a foil bearing results from a complex interaction of both internal and external factors. In a gas turbine engine environment, for example, a foil bearing's temperature would be influenced by its proximity to high temperature components, such as the combustor, compressor or turbine and the heat that it produces internally from the viscous shear occurring in the thin air film and any compression work. Even though the viscosity of air is low, the high surface speed required by the bearings for adequate load support coupled with a thin film results in a large

velocity gradient that generates a moderate amount of heat. The low thermal capacity of air makes it difficult for any appreciable amount of heat to be removed with side leakage leaving most to dissipate into the shaft and bearing. In fact, estimates place the heat absorbed by these two components at about 80% with the remaining 20% convected by side leakage (8). The end result is a shaft-bearing interface operating hotter than its immediate surroundings.

Breaking the energy distribution down further, it's expected that the shaft accepts a majority of this 80% because of its large exposed surface area and extension into cooler parts of the engine. The bearing's inability to dissipate its share of heat stems from its construction; specifically, the bump foils that enable its compliant nature. From a thermal viewpoint the bump foils isolate the top foil from the rest of the bearing because the support points are in line contact. This limits the conduction of energy which causes the thin top foil to quickly approach thermal equilibrium with the adjacent air film leaving most of the heat to flow into the shaft. Any heat that does pass through the bearing is controlled by thermal emission to the surrounding hardware and any energy transfer that does occur at the top foil/bump foil contact points.

If the localized temperatures grow unabated, bearing performance can be detrimentally affected in a number of ways. One concern is overheating of the bump foil material. Foil bearings are typically made from Inconel, a nickel based superalloy, because it retains an elastic modulus (spring rate) at high temperature better than most materials. However, as with most materials, it does experience a drop in its modulus with an ever increasing temperature. This softening effect increases the bearing's compliance, which reduces the bearing's maximum load capacity as demonstrated analytically and experimentally (9, 10). In addition, research suggests that changes to the bearing's stiffness (and possibly damping) properties will occur which can impact a system's rotordynamic behavior (11).

Foil bearings can also suffer from thermal runaway, a condition that usually leads to failure and is caused by a continuous increase in the bearing's preload. Preload in a foil bearing is obtained by designing the bearing's ID to be slightly smaller than the OD of the shaft, similar to an interference fit. When the top foil is manually retracted to allow its insertion onto the shaft, the bump foils elastically deform and produce reaction forces (preload) that push back against the shaft. This preload force acts over the entire top foil area. For manageable start-up torque, lift-off speed, and load capacity considerations, preload is typically around 6.89 to 10.34 kPa. Lighter preloads can adversely affect a bearing's stiffness and damping properties and, if low enough, can lead to rotor instability. On the other hand, a heavier preload will create higher start-up torque and lift-off speed requirements and a reduction in load carrying capacity. Because the shaft absorbs most of the heat during bearing operation, it expands faster than the bearing which increases the preload. This amplifies the stress on the fluid-film, much like an increase in the radial load, and leads to additional heat generation and further expansion of the shaft resulting in a self-sustaining cycle (thermal runaway) that will continue until the preload force overwhelms the fluid-film and high speed rubbing occurs (12). Understandably, bearing

types requiring an initially high preload for stiffness and damping considerations are more susceptible to this type of failure.

A third thermally induced problem is the formation of excessive axial thermal gradients across the bearing's half-width (middle to the edge). This phenomenon has been experienced during operation of most foil bearing types (overlapping leaf, multi-pad, single top foil) in the authors' lab and is especially prevalent in advanced, third generation (Generation III) bearings where the bump foils are designed to limit side leakage by stiffening the support at the bearing's edges. An excessive thermal gradient can sufficiently warp the top foil to the point that it interferes with the formation of a fully developed fluid-film. The cause for this phenomenon is hypothesized to be a circumferentially flowing slug of air that remains trapped in the middle of the bearing that undergoes continuous heating due to viscous shear (13). In fact, results from computer-based modeling of the fluid-film mass flow do provide credible evidence to support this theory (14). In a real application, non-uniform heating due to external sources can exacerbate the presence of these gradients and requires a thorough analysis to avoid dangerous levels. Of the three thermal related failure mechanisms, axial gradients are the most dangerous because the bearing can exhibit stable operation but fail when pushed to higher speed and/or load levels.

The importance of thermal management can best be elucidated by considering the report by Dykas who recounted a catastrophic bearing failure that produced a dime-sized hole in an Inconel journal (15). The amount of energy produced during the failure was substantial, considering the melting temperature of Inconel is around 1400 °C. Just before the failure, the 50.8 mm x 50.8 mm bearing was operating at a speed of 60 krpm in a 538 °C environment and supporting 222N load without active cooling. At this size and speed the bearing should easily support over 1700N based on the empirical rule-of-thumb equation for estimating load capacity for radial foil bearings (16). According to the report, computer-based structural modeling predicted that the failure was caused by the superposition of two phenomena, the first being point load deformation of the journal due to centrifugal forces from balance correction weights and the second being the presence of a large axial thermal gradient in the bearing. This combination produced a bulge in the journal that grew as it was continuously heated during operation until breaking through the air film, leading to a high-speed rub and bearing failure. As stated above, axial thermal gradients are a common occurrence in foil bearings and are an inherent trait stemming from their design and operating principle. Lab tests suggest that there is a risk of failure when they exceed approximately 22 °C/cm. This can happen in any ambient environment once the journal surface speed surpasses around 133 m/s but it depends upon other factors as well, such as type, preload, design, and length-to-diameter (L/D) ratio. For example, lab testing an L/D = 1, Generation III bearing in a room temperature environment with moderate preload (~6.89 kPa) and under low load experienced a destructive axial gradient when operating at speeds above 50 krpm and required active cooling to continue operation.

To address the need for thermal management in Oil-Free systems, the author previously tested the effectiveness of three techniques to control the viscous heat in radial foil bearings; direct

journal cooling, indirect journal cooling, and axial bearing cooling (17). The direct and indirect methods were designed to draw heat from the bearing by increasing the rate of thermal conduction through the journal. One advantage to this approach is that it addresses the journal growth due to thermal expansion and the resulting change in the bearing's preload force. The direct method impinged a jet of air on the inner surface of a hollow journal coincident with the bearing to maximize the convection coefficient and heat transfer. The indirect method of running air axially along the journal's inner diameter surface to increase the convection coefficient was less effective at bearing cooling. The test results proved that both techniques were successful at reducing bulk temperatures and axial thermal gradients but the direct method was more effective. The axial cooling technique, on the other hand, simulated the industry standard approach to thermal management by forcing air through the bearing's support structure (bump foils) to remove heat. This approach was also effective but results suggested that air flow rate and direction were important and, if not done with care, could exacerbate the development of an axial gradient to the point of bearing failure. This technique also runs the risk of increasing the bearing's preload and thermal runaway as direct cooling shrinks the bearing while the journal is expanding from the viscous heat, albeit at a slower rate. To minimize the risks, it is recommended that air be introduced into the hotter end of the bearing and at a flow rate that produces a more even axial temperature distribution. Applying any of these methods requires a thorough thermal analysis on the system to understand the temperature distribution in the bearing during operation, especially if it is located near a heat source. Given the choice of the three methods, direct journal cooling provides the most inherent benefits, but unfortunately, may be difficult or impossible to implement in most systems.

The operating principle behind hydrostatic gas bearings may provide an alternate, more useful approach to thermal management in foil air bearings. Hydrostatic bearings, whether radial or axial, depend upon a pressurized fluid injected into the bearing cavity to separate surfaces and provide load support. The pressure driven flow is also responsible for maintaining moderate bearing temperatures by removing the viscous heat produced in the fluid-film. Applying this concept to foil bearings operating in a gas turbine engine environment would require injecting air from one of the compressor stages directly into the middle of the circulating thin air film. Expected to be set-up as an open-loop arrangement, the heated air expelled from the bearing would then be piped through the engine to exit in the rear. This concept is similar to the approach reported by Kim and Park who integrated a hydrostatic capability into a radial foil bearing to alleviate the high start-up torque associated with large systems and to increase bearing load capacity (18). The hydrostatic function also demonstrated the ability to reduce bearing temperatures. However, there is no intent with this concept to reproduce a hydrostatic load carrying effect. Its only purpose is to provide thermal management control and is expected to be applicable to foil bearing designs using single or multiple top foils where space between foil(s) exist.

This report details a novel thermal management technique capable of reducing axial thermal gradients and bearing bulk temperatures by injecting air directly into the middle of the bearing to promote mixing with the hot circulating air film. The study was conducted on a Generation III bearing instrumented with three, type K thermocouples and an access hole for the injection air. The tests were conducted at room temperature and at various speeds while the bearing was supporting 222N. The technique was evaluated at two different injection mass flow rates, 0.017 kg/min and 0.051 kg/min.

2. Test Apparatus

Shown in figure 1 is the Generation III bearing used for the tests (19). The bearing has a nominal 50 mm inner diameter and a length of 41 mm. Temperatures were measured with three, type K thermocouples that were placed in the same axial plane, one in the middle (#2) and one on either side (#1 & #3) with a distance of 19 mm between #1 and #2 and 14 mm between #2 and #3. This distribution allowed monitoring of the axial temperature gradient that develops across the bearing's half-width. For a close approximation of the top foil temperature, the thermocouple was glued to the backside of a bump that was in contact with the top foil. The hole for air injection was located in the space between the free and fixed ends of the top foil and coincident with the middle of the bearing, placing it directly opposite from the load support region of higher pressure. Its orientation also directed the air to enter the bearing perpendicular to the circulating air film. No attempt was made, either analytically or experimentally, to ascertain the proper size, shape, or orientation of the hole to optimize results. In addition, a small amount of the top foil at the free end was removed with a high-speed grinding tool to provide an unobstructed path for the injection air to enter the bearing.

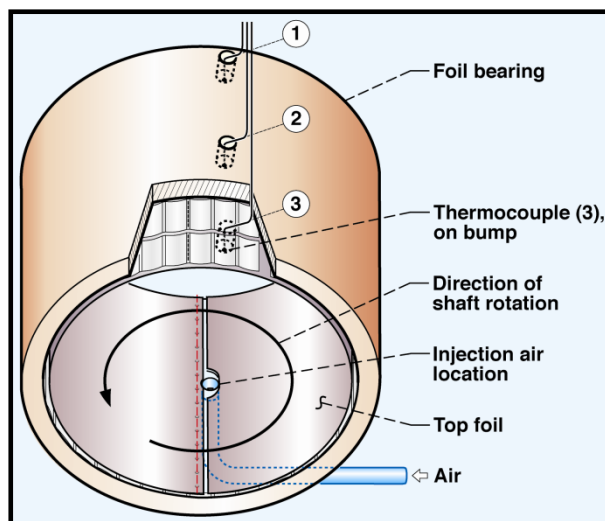


Figure 1. Schematic of the test bearing showing locations of thermocouples and inlet hole for air injection.

The set-up for the injection air delivery system is shown in figure 2 and consisted of steel and flexible plastic tubing and a 0.228 m³/min full scale flow meter supplied by 861.8 kPa shop air. The steel tube had an inner diameter of 2.9 mm and, with the smallest cross-sectional area, set the maximum amount of air deliverable to the bearing. A threaded fastener at the end of the steel tube screwed into the bearing holder and its tip extended into the injection hole in the bearing shell. Plastic tubing with an inner diameter of 4.3 mm was used to connect the flow meter to the air source and steel tube. A thermocouple inserted at the plastic tube/steel tube junction measured the air temperature before entering the bearing. With the flow meter control valve in its fully open position, the maximum flow rate was 0.068 kg/min

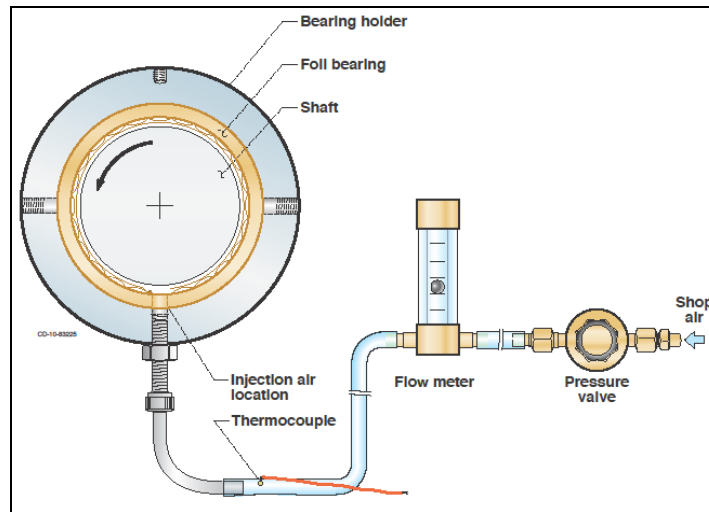


Figure 2. Hardware layout for injecting air into the bearing.

The normal, in-house procedure for preparing the test journal is to first plasma spray a high temperature, solid lubricant coating onto the journal surface and then heat treat it at 520 °C for 100 hr. Once cool, the journal is installed on the test rig and sized, using an in-place grinding system, to a final nominal diameter of 50.8 mm. After performing in-place, two-plane balancing to reach 50 krpm, the bearing and journal are together subjected to approximately 700 start-stop, break-in cycles under a 6.89 kPa load at 520 °C to produce a lubricious oxide surface layer and conforming surfaces (20).

The high-speed rig used to perform the tests is shown in figure 3 and is described in greater detail in reference 10. The rig consists of a main shaft supported by two ceramic, oil lubricated ball bearings in an overhung arrangement. An air impulse turbine attached to one end of the shaft is capable of driving the journal to a maximum rotational speed of 60 krpm. Radial loading of the foil bearing is accomplished via a vertical cable system with one end attached to the bearing housing in a stirrup configuration and the other to a pneumatic load cylinder mounted below the test rig. The rod extending from the bearing housing acts as a moment arm to relay the bearing torque to a load cell. The torque reading, however, was only used for health monitoring

as the air delivery system had an influence on the output. The furnace consists of two halves that surround the bearing for heating and also as a scatter shield for operational safety.

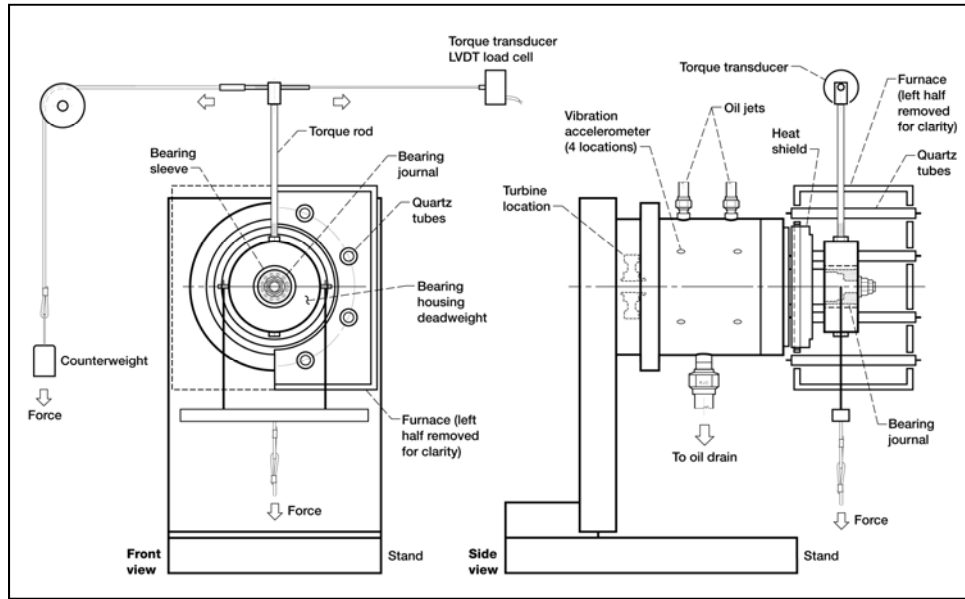


Figure 3. High-speed, high-temperature, journal foil air bearing test rig.

3. Procedure

Test preparation began by placing the bearing on the journal, attaching the air delivery system steel tube and radial loading cable to the bearing and then connecting the thermocouple leads. Once the scatter shield was in position and the data acquisition system started, the rig was accelerated to the test speed and the load applied. This condition was maintained for about 10 min to allow bearing temperatures to reach steady-state before air introduction. The first flow rate of 0.017 kg/min was injected into the bearing and held until the temperatures reached steady-state. The injection air flow rate was then tripled to 0.051 kg/min and the operating conditions maintained until temperatures again reached steady-state, at which time the data acquisition was stopped and the test concluded. This procedure was followed under room temperature conditions (23 °C) for speeds from 20 to 50 kprm while supporting 222N.

4. Test Results and Discussion

Overall test results are shown in table 1. For each test, the bearing temperatures and thermal gradients for injection flows of 0 (baseline), 0.017 and 0.051 kg/min are given. As demonstrated in the table the highest bearing temperatures were in the middle with the lower temperatures

occurring towards the edges. This temperature distribution is very common in this and other foil bearing designs along with the thermal gradient acting across the bearing's half width. As expected, bearing temperatures rose with increasing speed due to higher viscous shear. In fact, every temperature reading almost doubled when the speed went from 20 to 40 krpm. For each test condition, the response to air injection at 0.017 kg/min was almost immediate with a decrease in both bearing temperatures and thermal gradient but the change was small. The reaction was much more pronounced when the flow was tripled to 0.051 kg/min. An example of this behavior can be seen in figure 4 for the bearing operating at 30 krpm and supporting a 222N load. In this case, there was only a 3% and 2% decrease in the middle and edge temperatures, respectively, with an injection flow of 0.017 kg/min. However, at 0.051 kg/min, the decrease was 20% and 17%, respectively, demonstrating that bearing temperatures and thermal gradients can be managed through proper control of the injected air flow rate. The results also demonstrate the method's effectiveness is not localized to the middle of the bearing (coincident to the injection hole's location) but influences the entire bearing. It is not clear if the physical mechanism responsible for these results is due to displacing the retained slug of air in the middle of the bearing with a fresh, cooler supply or from fluid mixing. Additionally, it is unknown if the injected air is penetrating the air film sufficiently to directly cool the journal. Only through further in-depth experimental research or computer-based analytical modeling can these questions be answered.

Table 1. Bearing temperature results for the two injection air flows at three different operating speeds while supporting 222N. Injection air temperature = 23 °C.

	Injection Flow, kg/min	T₁, °C	T₂, °C	T₃, °C	Max Gradient, °C/cm
20 krpm	0	77.2	85.6	77.2	6.0
	0.017	77.4	83.9	77.4	4.6
	0.051	67.4	70.0	65.7	3.1
30 krpm	0	104.0	116.6	102.4	10.2
	0.017	102.2	112.7	100.6	8.7
	0.051	87.3	93.5	85.1	6.0
40 krpm	0	148.4	169.7	148.4	15.2
	0.017	146.4	164.5	146.4	12.9
	0.051	122.9	136.5	123.0	9.6

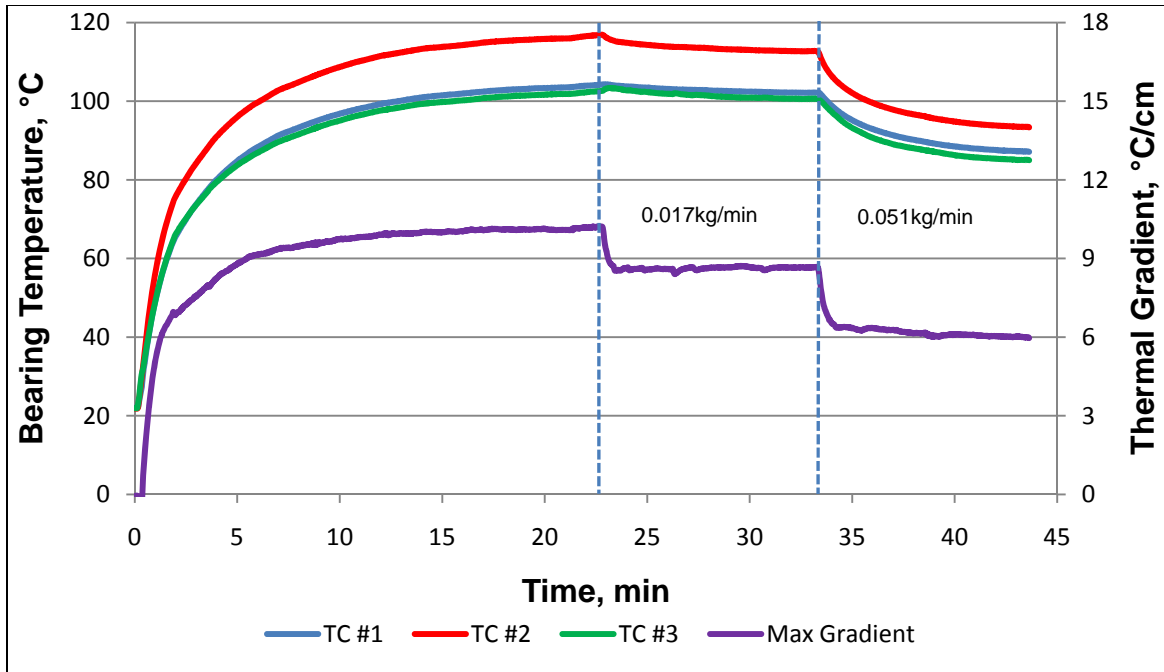


Figure 4. Time history plot of bearing temperatures and maximum axial thermal gradient showing the effects of applying air injection flows of 0.017 and 0.051 kg/min. Speed = 30 krpm, load = 222N.

The true effectiveness of injecting air as a thermal management technique was demonstrated when attempting to conduct tests at the highest speed. When testing the bearing operating at 50 krpm and supporting 89N (excessive test rig vibrations prohibited higher radial loads at this speed), the bearing temperatures did not reach steady-state but continued to rise along with the thermal gradient that neared 30 °C/cm, which is a dangerous level. A plot of bearing temperatures is shown in figure 5. Concurrently, there was also a slow increase in bearing torque and a corresponding drop in operating speed, symptoms of impending failure. An attempt was made to prevent the failure by first injecting 0.051 kg/min into the bearing at the 3.5 min mark, then 0.068 kg/min of air a minute later to reduce the gradient. Unfortunately, this was unsuccessful and the test was discontinued at the 5 min mark to avert failure and possible bearing and journal damage. Once the bearing had cooled, a second attempt at completing the test was made by injecting the maximum flow rate of 0.068 kg/min at the start to control the gradient. This approach was successful as it prevented the gradient from growing to excessive levels. As shown in figure 6 bearing temperatures reached steady-state with the middle temperature at 192 °C and the other two were approximately 174 °C. The thermal gradient remained low and fluctuated around 12 °C/cm. This test demonstrated that injecting air into the circumferential flow stream is an effective thermal management technique that allows foil bearings to operate at conditions that would otherwise result in failure.

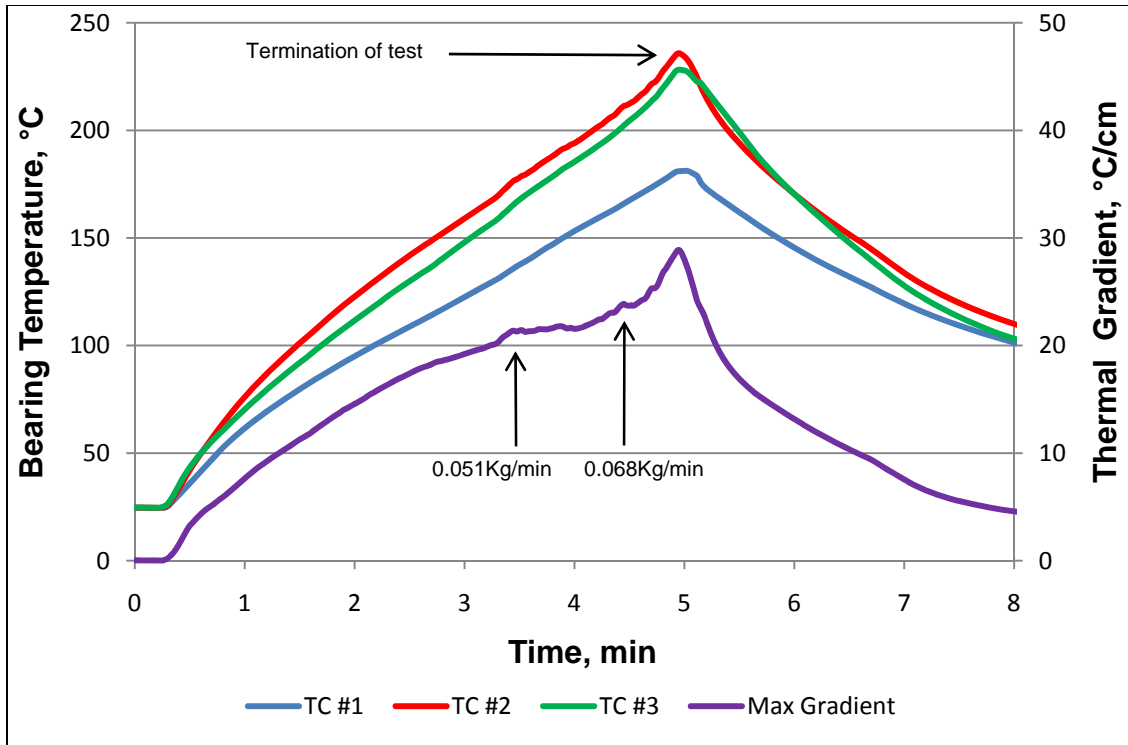


Figure 5. Bearing temperatures demonstrating an excessive thermal gradient situation. Injection air at 0.051 kg/min was delivered at the 3.5 min mark followed by 0.068 kg/min at the 4.5 min mark. Test was discontinued once the thermal gradient surpassed 25 °C/cm. Speed = 50 krpm. Load = 89N.

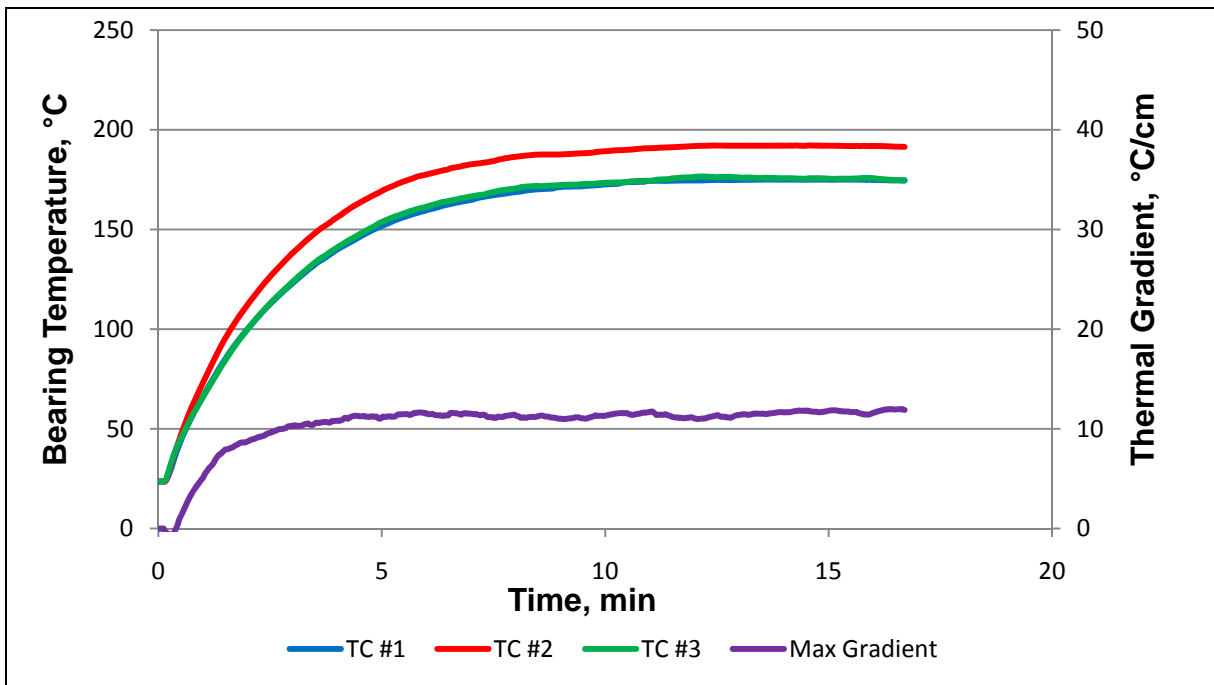


Figure 6. Repeat of operating conditions that led to failure (figure 5) except a constant air injection of 0.068 kg/min was applied at the beginning of the test. Speed = 50 krpm. Load = 89N.

Unlike testing in the lab where the radial load remains fixed in the same circumferential location, a foil bearing operating in a real application, such as in a gas turbine engine on a helicopter, is required to support dynamic loads in any direction based on the resultant vector summation of rotor weight and gyroscopic forces produced during any flight maneuver. To address this issue, tests were devised to evaluate if the angular distance between the load support region and the point of injection either contributes to or deters from the method's effectiveness. Changes to this distance affect the time available for the incoming air to either mix or displace the existing air film. Two tests were performed at room temperature with the bearing operating at 20 krpm and supporting 89N. Adjusting the hole location was accomplished by unscrewing the threaded fastener for the steel tube, rotating the bearing in its deadweight housing to line up the injection hole with pre-drilled, threaded holes, and reinstalling the fastener (see figure 2). The first test was performed with the injection hole 90° before the high pressure zone (upstream) and the second test with the hole 90° after the high pressure zone (downstream). Results are shown in table 2. For the upstream case the bearing pre-test temperature was a uniform 23.4 °C but, after operating for 10 min, bearing temperatures rose with the middle reaching approximately 76.1 °C and 69.2 °C at the edges (nos. 1 & 3), resulting in a 5.0 °C/cm thermal gradient. Injecting air at 0.051 kg/min dropped the middle temperature to 59.8 °C and the edges to approximately 56.0 °C with the gradient leveling off at 3.1 °C/cm. At the beginning of the downstream test, the bearing temperature was a uniform 20.8 °C but rose to 71.9 °C in the middle, 68.0 °C at the edges with a 2.8 °C/cm gradient, close to the preceding test. After 10 min of injecting 0.051 kg/min of air the bearing temperatures reached steady-state with the middle at 57.3 °C and the edges 55.6 °C. The gradient was 1.2 °C/cm. A comparison of the upstream and downstream test results does not show any significant differences in bearing temperatures, therefore suggesting that the method's effectiveness is not a function of injection location.

Table 2. Effect of air injection location with respect to the load support region on bearing temperatures and thermal gradient. Speed = 20 krpm. Load = 89N. Injection air temperature = 22 °C.

	Injection Flow, kg/min	T₁, °C	T₂, °C	T₃, °C	Max. Gradient, °C/cm
90° Upstream	0	23.4	23.4	23.4	-
	0	69.2	76.1	69.2	5.0
	0.051	56.6	59.8	55.4	3.1
90° Downstream	0	20.8	20.8	20.8	-
	0	68.0	71.9	68.0	2.8
	0.051	55.6	57.3	55.6	1.2

5. Conclusion

Test results suggest that injecting air into the circulating thin film of a foil bearing is a viable thermal management technique at controlling bearing bulk temperatures and thermal gradients. It is not, at the injection flow rates used here, as effective as other methods demonstrated by the author in the past, but room for improvement exists and may be more easily implemented. Test results also suggest that injection location, with respect to the load support region, does not impact the effectiveness of the technique.

Because there was no attempt to optimize the technique's effectiveness, additional research on method of air delivery should be performed before implementing this approach. Specifically, the hole quantity, size, geometry (oval, round), and orientation (angled to deliver the air with or against the circulating air film) should be investigated. Lastly, foil thrust bearings use a number of individual, sector-shaped pads spaced evenly around a circular plate. With ample space between the pads foil thrust bearings would likely benefit from this type of thermal management approach.

6. References

1. Blok, H.; van Rossum, J. J. The Foil Bearing-A New Departure in Hydrodynamic Lubrication. *Lubrication Engineering* **1953**, 9 (6), 316–320.
2. Emerson, T. P. The Application of Foil Air Bearing Turbomachinery in Aircraft Environmental Control Systems. in *Proc. of the ASME Intersociety Conference on Environmental Systems*, San Diego, CA, Paper No. 780-ENAS-18, 1978.
3. Advanced Gas Turbine (AGT) Technology Development, NASA CR-165175, 1979.
4. Suriano, F. J.; Dayton, R. D.; Woessner, F. G. Test Experience with Turbine-End Foil Bearing Equipped Gas Turbine Engines. *ASME 28th International Gas Turbine Engine Conference*, Phoenix AZ, March 27–31, 1983.
5. Lubell, D.; DellaCorte, C.; Stanford, M. Test Evolution and Oil-Free Engine Experience of a High Temperature Foil Air Bearing Coating. *Proceedings of the GT2006: ASME Turbo Expo 2006*, Barcelona, Spain, GT2006-90572, 2006.
6. Larue, G.; Kang, S.; Wick, W. Turbocharger with Hydrodynamic Foil Bearings. Patent #7,108,488, 2006.
7. Heshmat, H.; Walton, II, J. F.; Tomaszewski, M. J. *Demonstration of a Turbojet Engine Using an Air Foil Bearing*; ASME Paper GT-2005-68404; presented at the ASME Turbo Expo 2005, Power for Land, Sea and Air, Reno-Tahoe, NV, 2005.
8. Salehi, M.; Swanson, E.; Heshmat, H. Thermal Features of Compliant Foil Bearings-Theory and Experiments. *ASME journal of Tribology* **2001**, 123, 566–571.
9. Heshmat, H.; Walowit, J.; Pinkus, O. Analysis of Gas-Lubricated Foil Journal Bearings. *ASME Journal Lubrication Tech Trans.* **1983**,105 (4), 638–646.
10. DellaCorte, C. *A New Foil Air Bearing Test Rig for Use to 700 °C and 70,000 rpm*; NASA TM 107405; 1997.
11. Howard, S.; DellaCorte, C.; Valco, M.; Prael, J. Steady-State Stiffness of Foil Air Journal Bearings at Elevated Temperatures. *STLE Tribology Transactions* **2001**, 44 (3), 489–493.
12. Radil, K.; Howard, S.; Dykas, B. The Role of Radial Clearance on the Performance of Foil Air Bearings. *STLE Tribology Transactions* **2002**, 45 (4), 485–490.
13. Radil, K.; Zeszotek, M. An Experimental Investigation into the Temperature Profile of a Compliant Foil Air Bearing. *STLE Tribology Transactions* **2004**, 47 (4), 470–479.

14. Carpino, M.; Talmage, G. A Fully Coupled Finite Element Formulation for Elastically Supported Foil Journal Bearings. *STLE Tribology Transactions* **2003**, *46* (4), 560–565.
15. Dykas, B.; Howard, S. Journal Design Considerations for Turbomachine Shafts Supported on Foil air Bearings. *Trib. Trans.* **2004**, *47*, 508–516.
16. DellaCorte, C.; Valco, M. Load Capacity Estimation of Foil Air Journal Bearings for Oil-Free Turbomachinery Applications. *STLE Tribology Transactions* **2000**, *43* (4), 795–801.
17. Radil, K.; Zeszotek, M. Thermal Management Techniques for Oil-Free Turbomachinery Systems. *STLE Tribology Transactions* **2007**, *50* (3), 319–327.
18. Kim, D.; Park, S. Hydrostatic Air Foil Bearings: Analytical and Experimental Investigation. *Tribology International* **2009**, *42*, 413–425.
19. Heshmat, H. High Load Capacity Compliant Foil Hydrodynamic Journal Bearing. U.S. Patent No. 5,988,885, 1999.
20. Radil, K. C.; DellaCorte, C. *The Effect of Journal Roughness and Foil Coatings on the Performance of Heavily Loaded Foil Air Bearings*; NASA TM-2001-210941; 2001.

No. of Copies	Organization
1 ELEC	ADMNSTR DEFNS TECHL INFO CTR ATTN DTIC OCP 8725 JOHN J KINGMAN RD STE 0944 FT BELVOIR VA 22060-6218
2	NASA GLENN RSRCH ATTN RDRL VTP B SELJAN MS 21-2 21000 BROOKPARK RD CLEVELAND OH 44135
20	NASA GLENN RSRCH ATTN RDRL VTP K RADIL MS 23-2 21000 BROOKPARK RD CLEVELAND OH 44135
1	US ARMY RSRCH LAB ATTN RDRL CIM G T LANDFRIED BLDG 4600 ABERDEEN PROVING GROUND MD 21005-5066
3	US ARMY RSRCH LAB ATTN IMNE ALC HRR MAIL & RECORDS MGMT ATTN RDRL CIM L TECHL LIB ATTN RDRL CIM P TECHL PUB ADELPHI MD 20783-1197

TOTAL: 27 (1 ELEC, 26 HCS)

INTENTIONALLY LEFT BLANK.